Journal of Thermal Engineering
Web page info: https://jten.yildiz.edu.tr
DOI: 10.18186/thermal.991095

Research Article

Influences of the dead end on the flow characteristics at the exhaust manifold of a marine diesel engine

Gorkem BENEK[1,2,*], Osman Azmi OZSOYSAL[1,*]

[1]*Department of Naval Architecture and Ocean Engineering, Istanbul Technical University, Istanbul, Turkey*
[2]*Department of Marine Sciences, Ordu University, Ordu, Turkey*

ARTICLE INFO

Article history
Received: 31 December 2019
Accepted: 16 July 2020

Key words:
Exhaust manifold; Dead end; Computational fluid dynamics; Pressure distribution

ABSTRACT

A 3D Computational Fluid Dynamics (CFD) model of an exhaust manifold with and without a dead end has been developed to investigate the impacts of its geometry on the flow structure and the pressure distribution within the manifold. The model differs from previously studied models principally for its ability to approach the realistic operating principle of an engine as the modelled exhaust valves of the investigated engine open and close according to the firing order. The experimental results of an exhaust manifold without a dead end has been used to validate the CFD model through the pressure distribution and the flow structure. The outcomes demonstrated that the developed CFD model concurred well with the experimental data. The effects of the dead end on the exhaust manifold were then investigated using the validated CFD model. The study has revealed that the addition of a dead end (i) provides a smoother pressure distribution inside the manifold and increase in the efficiency of the turbocharger and (ii) decreases the pressure inside of the interconnection pipes of cylinders while the exhaust gas discharges. Moreover, the results disclose a smoother discharge of exhaust gases leading to a more effective sweeping of the exhaust gas thorough the cylinder without causing any exhaust backpressure. Furthermore, the dead end reduces the turbulence kinetic energy at the blind end of the exhaust manifold resulting in a decrease of pressure loss within. The abovementioned findings regarding to the flow structure and the pressure distribution within the exhaust manifold improve the efficiency of the engine.

Cite this article as: Gorkem B, Osman A. Influences of the dead end on the flow characteristics at the exhaust manifold of a marine diesel engine. J Ther Eng 2021;7(6):1519–1530.

INTRODUCTION

The performance of the exhaust manifold directly affects the efficiency of the diesel engine [1–3]. Ozsoysal [4–5] conducted an experimental study on the effects of the exhaust manifold on the efficiency of the engine. In his study, Ozsoysal [5]observed that the flow structure and pressure fluctuations in the exhaust manifold affect the sweeping since the exhaust gases in the cylinders encounter

***Corresponding author.**
*E-mail address: gbenek@itu.edu.tr, ozsoysal@itu.edu.tr

This paper was recommended for publication in revised form by Regional Editor Bekir Şener

high pressure in the manifold during the exhaust valves are opened. The inefficient sweeping then affects the combustion efficiency in the cylinders. Thus, the overall engine performance. Ozsoysal [5] discussed that the reason could be the manifold geometry. The present study aims to investigate the impacts ofthe exhaust manifold geometry on the flow structure of exhaust gases and pressure distribution in the exhaust manifold.

Recent studies research the exhaust manifold design to improve the engine performance via methods that can mainly be classified into two groups: chiefly, experimental and numerical methods. In the experimental studies, accurately measuring pressure, velocity and turbulence values as a function of time can be arduous due to the high kinetic energy and the temperature of gases. Furthermore, it is also difficult to approximate or simulate the real turbulence characteristics in the system. Besides, the devices used to collect the data, and the prototypes used in the experiments could constitute a financial difficulty [6]. Hence, the Numerical models have been developed to reduce the number of experiments and costs. Computational Fluid Dynamics (CFD) is widely employed in diverse engineering applications due to its ability to capture more details of flow structure [7–8]. It is also frequently utilized in the development of internal combustion engines and the reduction of emissions [9]. The three-dimensional (3D) numerical analysis gives better results when analyzing the flow dynamics of emission-reducing components such as suction and exhaust manifolds, SCR, DPF, and geometric optimization [10–11].

Zhang et al. [12] investigated two different exhaust geometries with 1D and 3D mixed models. They reduced the turbulence and pressure losses in the manifold with the improvements in its geometry. They also decrease the amount of residual gas by obtaining a better discharge of burnt gases within the cylinder. The pump work done by the piston for sweeping the exhaust gases is also affected by flow dynamics.

The exhaust manifold design as well as the flow dynamics in the exhaust have a direct and significant influence on the engine performance and emissions. Occurences such as backflow and backpressure to the cylinder, when the exhaust valves are opened, are strictly related to flow dynamics. Payri et al. [13] experimentally investigated the flow dynamics of the exhaust gas at the junction points of the exhaust manifold. They suggested a method that can predict the dynamic movements of pressure waves in pipes in the 1D model.

The flow dynamics affect the volumetric efficiency. Parts of the exhaust system, such as valves, manifolds, and also the firing order are the main determinants of the exhaust flow dynamics. Emara et al. [14] examined the flow in the manifold by opening the exhaust valves of a six-cylinder diesel engine as couples. A new manifold was designed via examining the pressure drop and the uniformity of the flow structure.

Turbulence occurs when exhaust gases leave the cylinder with a high energy and velocity. That results in pressure loss and the deterioration of the flow uniformity. The turbulence-free flow was investigated by Hinterberger and Olesen [15]. They analysed the effects of flow on the exhaust manifold and SCR systems by determining flow uniformity and pressure loss as constraint functions. The pulsating flow of gases in the exhaust manifold as well as the deterioration of the flow uniformity as a result of the turbulence, adversely affect the emission reduction systems. Siqueira et al. [16], on the other hand, examine the turbulent flow in steady state by CFD method and showed the effects of flow uniformity and flow structure on the cylinders.

Exhaust gases carry high energy because of their high temperature and pressure. Therefore, the volumetric efficiency of the engine increases when the exhaust gases are utilized in the turbocharger rather than being directly disposed to the atmosphere. In order for the turbo charge compressor to operate efficiently, it is essential that the gas flows through the fins is uniform or as straight as possible. Xu et al. [17] investigatethe pressure drop in the exhaust manifold of the gasoline engine. Their results emphasized the need to develop a new and better manifold design. In order to reduce the pressure loss caused by the pulsating flow and turbulence, the exhaust manifold and pipes must be well designed geometrically. Umesh et al. [18] investigate the effect of manifold geometry on volumetric efficiency and backpressure to optimize multi-cylinder SI engine. Their study resulted an increase in volumetric efficiency.

Backpressure can occur in the exhaust system due to the geometric structures of the manifold, valves and cylinder connection channels as well as the effect of exhaust gas dynamics. Moreover, the backpressure is vital to engine's performance and efficiency. Rajadurai et al. [19] studied both experimentally and computationally showed that the difference up to 60% existed between backpressure values in cold and hot gas flows. Backpressure results in a decrease in the efficiency of the internal combustion engine, therefore a rise in the fuel consumption. Ma et al. [20] have optimized the exhaust manifold geometry with a1D model. During the optimization, they increased the length of the connection pipes. As a result, the effects on other cylinder connections were reduced. Thus, the engine efficiency was arisen by reducing the backflow and the backpressure.

It has been observed that manifold geometry affects directly the diesel engine overall performance. It makes the gas flow pattern and dynamic variables such as the velocity, the pressure and the temperature to change from point to point locally throughout the exhaust manifold. Some not well-designed manifold geometries also cause the abnormal running performance of one or two cylinder, arbitrarily.

Pressure and temperature variations inside those cylinders differ much more than others'. Abnormal running of one or more cylinders cause fatal errors and hazards. It has been seen that many studies haven't included the dead end effects on the overall engine performance characteristics. Mostly, in the literature, studies deal with the effects of the size and geometry of the branched type exhaust manifold on the turbocharger efficiency or exhaust emission characteristics. However, the dead end offers an important selection to arrange/rearrange the wave pressure fluctuation throughthe manifold by absorbing or reflecting to damp the gas pressure and velocity.

In the present study, 3D CFD models of a marine diesel engine exhaust manifold have been developed to investigate the effects of the exhaust manifold geometryon the flow structure and the pressure distribution within. Moreover, the effects of the exhaust gases, which are discharged from cylinders according to the firing order, on flow structure were examined. The first model, exhaust manifold without a dead end, is designed as the exhaust manifold mentioned in Ozsoysal [4–5]. This model was then verified using the mass flow rate of exhaust gases and the pressure distribution in the exhaust manifold in experimental studies [4–5]. A dead end has then been added to the mentioned 3D CFD model in order to change the exhaust manifold geometry and investigate the effects of the dead end on the flow structure and the pressure distribution inside the exhaust manifold. The simulation results of exhaust manifolds having and lacking a dead end have then been compared and the performance of the exhaust manifold having and lacking a dead end has been examined.

Analyses and comparisons were based on pressure and temperature variations with time along the exhaust manifold. Its general curve characteristics and trends of graphs were found similar and the average values (pressure & temperature) of 3D modelling at any section of the manifold almost matched with data in literature (4, 5). Thus, the present study endeavours find suitable and acceptable answers to questions like how the geometry of dead end in 3D modelling affect the discharging mass from cylinders, how flow pattern changes around the ports and throughout the manifold, if there is any backflow into the cylinders, etc.

It should be noted that the effect of the residual gases in the cylinders on volumetric efficiency as well as the combustion in the cylinders are out of scope for this study. The paper investigates how the dead end affects the flow pattern in the exhaust manifold.

It should also be noted that there are some restrictions about the validations due to some circumstances as to find any opportunity to make some tests on the same marine diesel engine with and without several type dead end due to the financial and manufactural problems. In addition, the engine manufacturers prefer not to share the detailed data about their productions due to commercial privacy.

MATHEMATICAL MODEL

Governing Equations

In order to obtain the flow structure within the exhaust manifold, continuity, momentum and energy conservation laws are used applied. The equations of a continuum fluid are governed by a set of partial differential equations known as the Navier-Stokes equations [21]. For the fluid behaving as an ideal gas, the equations can be expressed as:

$$\frac{\partial p}{\partial t}+\nabla\left(\rho v\right)=0 \tag{1}$$

$$\frac{\partial}{\partial t}[\rho v]+\nabla\{\rho vv\}=\nabla\{\mu\nabla v\}-\nabla p +\nabla\{\mu(\nabla v)^{T}\}-\frac{2}{3}\nabla\left(\mu\nabla v\right)+f_b \tag{2}$$

$$\frac{\partial}{\partial t}\left[\rho c_p T\right]+\nabla\left\{\rho c_p vT\right\} =\nabla\left[k\nabla T\right]+\rho T\frac{Dc_p}{Dt}+\frac{Dp}{Dt}-\frac{2}{3}\mu+\mu+\dot{q}_v \tag{3}$$

where the energy equation (eq. 1) appears in terms of temperature. Equations 2 and 3 display the momentum and continuity equations, respectively. The set of equations should be affixed by an equation of state pertaining density to temperature and pressure for an ideal gas is given by

$$\rho=\frac{p}{RT} \tag{4}$$

The turbulence equation is crucial for the simulation of the exhaust manifold. The shear stress transport (SST) k-ω model, developed by Menter [22], is a popular model that is successfully applied to simulate a wide range of turbulent flows [23]. The SST k-ω model is reduced to the k-ε model [24] in free stream layer and the k-ω model [25] close to the wall. In the SST k-ω model, k and ω are obtained by solving:

$$\frac{\partial k}{\partial t}+U_j\frac{\partial k}{\partial x_j}=P_k-\beta^{*}k\omega+\frac{\partial}{\partial x_j}\left[\left(\nu+\sigma_k\nu_T\right)\frac{\partial k}{\partial x_j}\right] \tag{5}$$

$$\frac{\partial \omega}{\partial t}+U_j\frac{\partial \omega}{\partial x_j}=\alpha S^2-\beta\omega^2+\frac{\partial}{\partial x_j}\left[\left(\nu+\sigma_\omega\nu_T\right)\frac{\partial \omega}{\partial x_j}\right] +2(1-F_1)\sigma_{\omega^2}\frac{1}{\omega}\frac{\partial k}{\partial x_i}\frac{\partial \omega}{\partial x_i} \tag{6}$$

Where F_1 is the blending function. F_1 is equal to 1 inside the boundary layer, and to 0 in the free stream. P_k is the production limiter; ν_T is the kinematic eddy viscosity. σ_{k1}, σ_{k2},

$\sigma_{\omega 1}$, $\sigma_{\omega 2}$, β_1, β_2, β^* are constants taking the values 0.85, 1, 0.5, 0.856, 0.075, 0.0825, 0.09, respectively [26].

NUMERICAL SET-UP

Geometry of the Exhaust Manifold

Two exhaust manifold geometries of a high speed, turbocharged marine diesel engine have been investigated in this studyand are shown in Figure 1. The dimensional unit in the figure is in millimeters. The main difference between the two manifolds is that one has a dead end (Figure 1 b) while the other does not (Figure 1 a).

Solution Algorithm

In this study, compressible RANS equations have been solved by Open FOAM software. PIMPLE algorithm has been used for the calculation of the pressure and velocity values that allows the use of PISO and SIMPLE algorithms together. PISO algorithm is an iterative solver and applied for transient cases. PIMPLE algorithm is utilized for steady state cases. In PIMPLE algorithm, SIMPLE algorithm is executed for every time step, where outer correctors are the iterations, and once the solution converges, it will move on to the next time step. Therefore, a better stability is reached from PIMPLE over PISO. In the PISO algorithm, the density value has been obtained by using the pressure and temperature values as initial values in the equilibrium equation. The acquired value is applied to the pressure correction equation, which is derived from the continuity equation, and then the pressure and velocity values are calculated from the pressure correction equation. Finally, the energy and turbulence equations are solved. Small time steps are required to solve the PISO algorithm. The main reason for studying with the PIMPLE algorithm is to increase the time steps to shorten the solution process. The momentum and pressure values between the time steps are solved using the SIMPLE algorithm in order to minimize the residuals and approach to the absolute solution.

Engine Specification Set Up

The modelled engine in this study bears the same specifications as the engine used by Ozsoysal [4–5] and is a 16-cylinder V-type turbocharged, high-speed marine diesel engine. Each cylinder block has two manifolds, namely an exhaust and an inlet manifold. Four highly sensitive piezoelectric transducers, suitable for the high pressures, are used to measure the gas pressure inside the cylinders and are mounted over the combustion bowl and flushed into the fire deck. Four piezoelectric transducers with low sensitivity, suitable for only low pressures, are used to measure the gas pressure inside the manifold pipes and are mounted to approximately the middle of the manifold pipes. The engine runs at 1900 rpm with a barometric pressure of 0.98 bar. The stroke/bore ratio and compression ratio of the engineare 1.1212, and 12.3, respectively. The engine has a firing order of 5-2-8-3-4-6-1-7. The fuel has a calorific value of 42800 kJ/kg, and a carbon fraction ratio of 0.8672. Finally, the mechanical efficiency is 0.90.

Mesh Calculation

The number of cells has been checked for independence in order to ensure that calculations are not affected by the cell size. Domain mesh consisting of hexahedra and polyhedra cells is applied as the manifold model as shown in Figure 2.

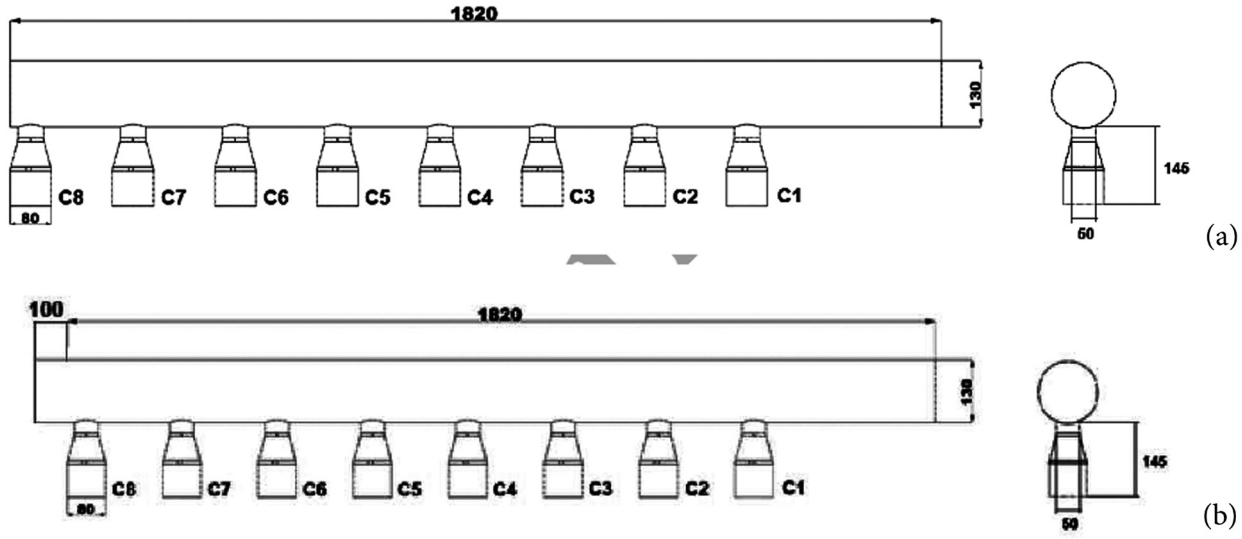

Figure 1. Exhaust Manifold of the Marine Diesel Engine. (**a.** without a dead end **b.** with a dead end).

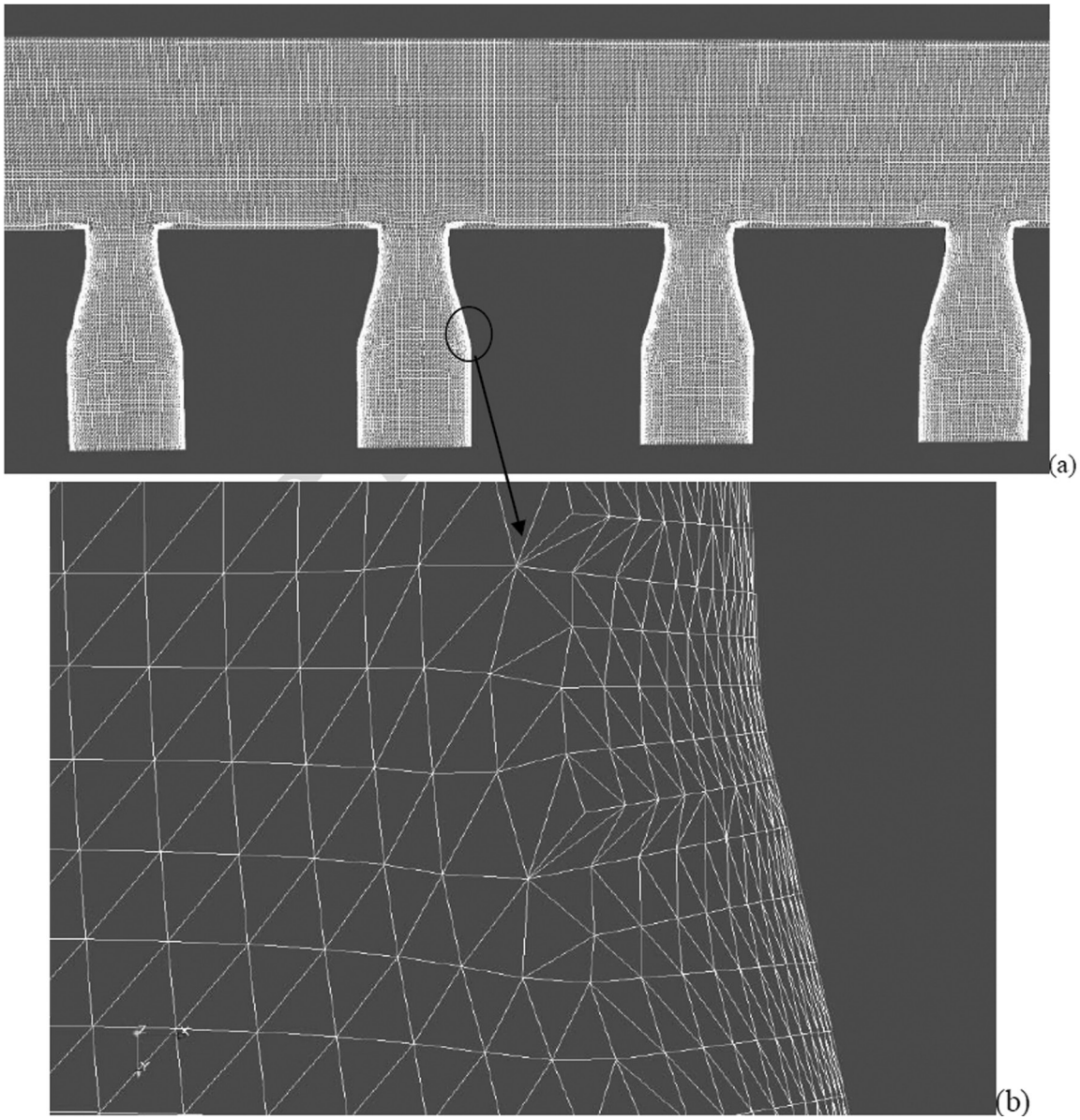

Figure 2. Mesh Quality of the Exhaust Manifold (**a.** Manifold view **b.** Detailed mesh view).

The model has been tested for three different mesh sizes (namely1.3M, 1.8M and 2.3M) to improve and to check the sensitivity levels of the results. As shown in Figure 3, there is an error rate of less than 2% among the results in the exhaust manifold. Significant difference was not observed between medium and fine mesh, whereas coarse mesh produced relatively distant results from the other two cases. When considering the power of the computer and the solution time, it has been seen that the medium mesh would give satisfactory results as shown in Figure 3. Therefore, this mesh structure and topology have been used in all subsequent analyses. The time-step has been adjusted with a constant Courant number of 0.15–0.3, which was set to 10^{-7} s.

Boundary Conditions

No-slip boundary condition has been assumed at the walls with zero-gradient boundary condition for all hydrodynamic variables. Inlet-outlet pressure boundary condition has been selected for the outlet boundary condition.

To compare the simulation results with Ozsoysal's experimental results [4–5], the temperature of the exhaust gas obtained by Ozsoysal [4–5], which is 1385 K, has been applied as the inlet temperature boundary condition for each inlet. Two mass flow rateshas been applied as the inlet mass flow boundary conditions depending on the exhaust valves state. For crank angles within each cylinders where the exhaust valves are open a mass flow rate of 0.1956 kg / s,

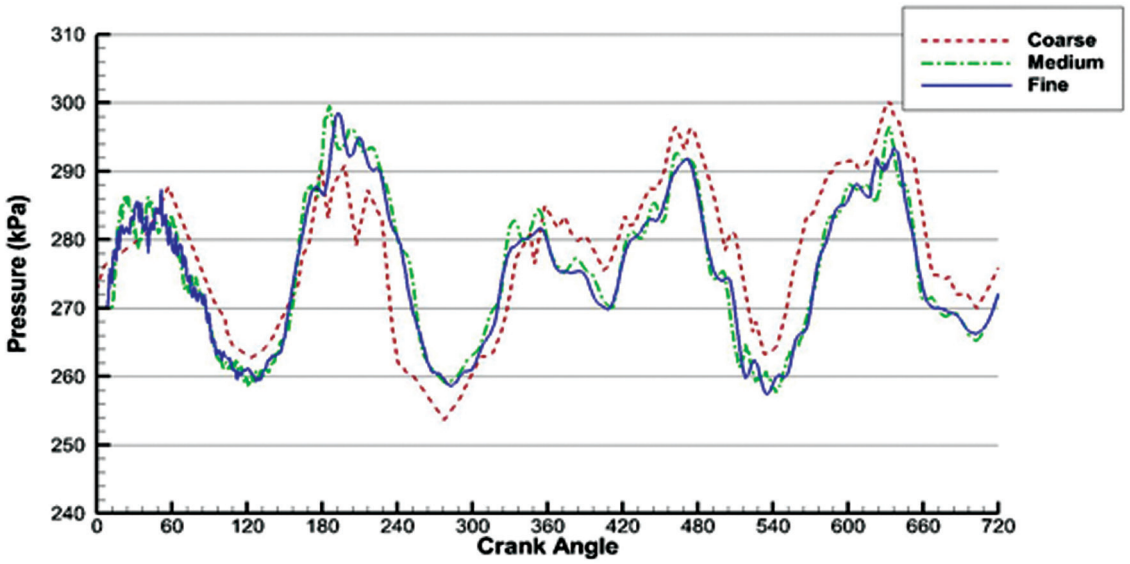

Figure 3. Pressure Distribution at Exhaust Manifold for Mesh Dependency.

Table1. EVO and EVC crank angles of cylinders according to firing order

	Cylinder5	Cylinder2	Cylinder8	Cylinder3	Cylinder4	Cylinder6	Cylinder1	Cylinder7
EVO	0^0 CA	135^0 CA	190^0 CA	315^0 CA	405^0 CA	450^0 CA	585^0 CA	630^0 CA
EVC	337^0 CA	472^0 CA	517^0 CA	652^0 CA	742^0 CA	787^0 CA	922^0 CA	967^0 CA

obtained from Ozsoysal's experimental data [4–5], has been used. These crank angles, exhaust valve opening (EVO) and exhaust valve closing (EVC), for each cylinder are given in Table 1according the firing order. For all other crank angles, where the exhaust valves are closed, a mass flow rate of 0 kg/s has been taken. As shown in Table 1, the exhaust valves of cylinder 5 are opening first according to the firing order and the relative exhaust valve opening (EVO) is assumed to be 0^0 CA.

VALIDATION OF SIMULATION

The simulation results of the developed 3D CFD model have been compared to the experimental results of Ozsoysal [4–5] in order to verify their accuracy. It should be noted that the boundary condition data used in this 3D CFD analysis are obtained from the studies of Ozsoysal [4–5].

As the flow in the exhaust manifold has an unsteady behaviour, the 3D CFD simulation calculations have been carried on three power cycles (3*720 CA) in order to stabilise the flow in the manifold. Once the stabilisation of the flow has been reached, the pressure values in the manifold have been compared with the experimental data in the research of Ozsoysal [4–5]. As shown in Figure 4, the pressure distribution in the exhaust manifold for the numerical simulation displays a variation of less than 2% compared to the pressure distribution for the experimental results. It can be concluded that these simulations results agree well with the experimental results.

RESULTS AND DISCUSSION

The developed 3D CFD model was run for two different simulation geometries, namely, with and without a dead end in the exhaust manifold. As a result, the pressure distributions and the turbulence kinetic energy values in the exhaust manifolds were acquired at different crank angles. Figures 5, 6, 7, and 8 display the pressure distributions at respectively 252, 256, 261, $331CA^0$ while Figures 9 and 10 show the turbulent kinetic energy values at respectively 331 and $419CA^0$.

As shown in the Figure5, the pressure values in the connection pipes of the exhaust manifold without a dead end are higher than the connection pipes of the exhaust manifold with a dead end. According to this figure, cylinder 8 is next to the blind end of the manifold, and cylinder 1 is closer to the turbocharger side. Whenever the exhaust valve of cylinder 8 is open, the discharge flow forces the gas inside the manifold to compress through the interconnection pipe

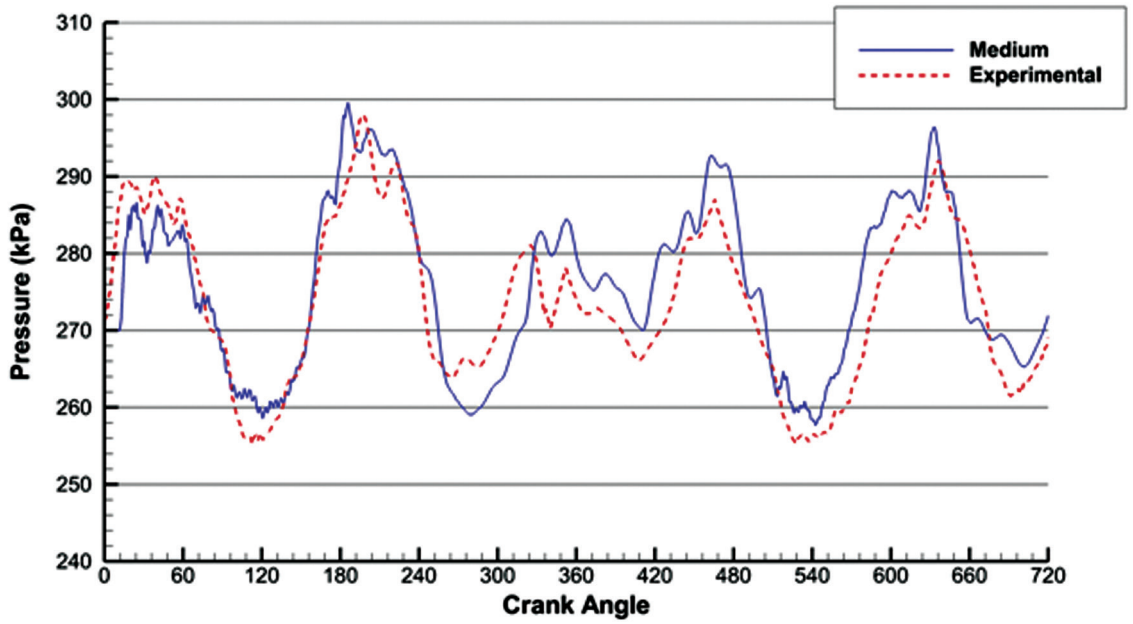

Figure 4. Pressure Distribution in the exhaust manifold for the Numerical Simulation and the Experimental Results.

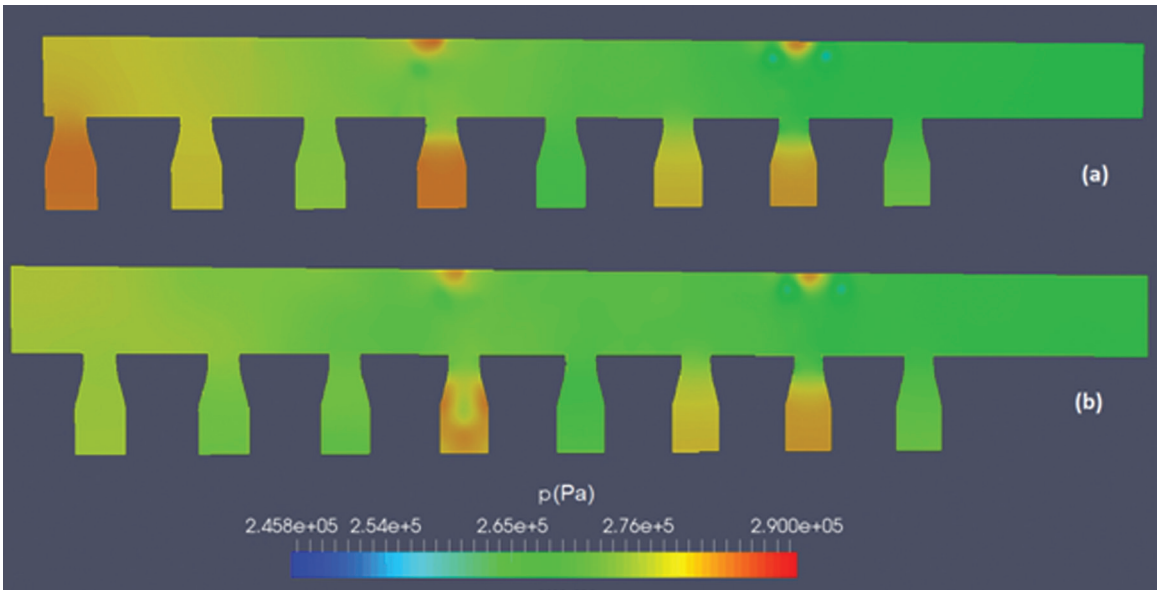

Figure 5. Pressure Distribution at 252 CA° (a. Original Manifold; b. Manifold with Dead End).

of cylinder 5. However, the pressure inside the interconnection pipe of the cylinder 5 drops significantly when utilizing a dead end. This occurs because of the reflected pressure waves from the dead end. The addition of a dead-end clearly provides a relatively smoother pressure distribution inside the manifold.

Figure 6 displays the pressure variation after 4°CA relating to the case in Figure 5. As shown in Figure 6, the exhaust gas hardly discharges from cylinder 8 due to the higher pressure inside the interconnection pipe at the exhaust manifold without a dead end. However, the addition of a dead end easily helps to drop the pressure inside the exhaust manifold. In addition, the new pressure distribution formed in the manifold after the addition of the dead end induces the pressure in the connection pipe of the cylinder 5 and 8 to decrease.

Approximately 5°CA later, Figure 7 illustrates that the pressure in the exhaust manifold without a dead end

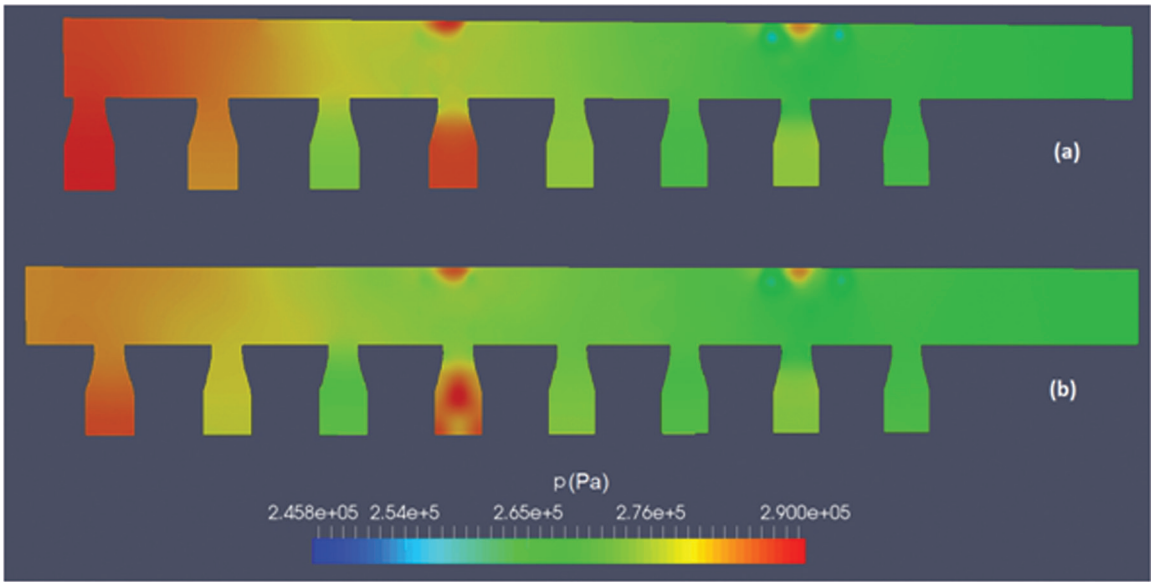

Figure 6. Pressure Distribution at 256 CA° (**a.** Original Manifold; **b.** Manifold with Dead End).

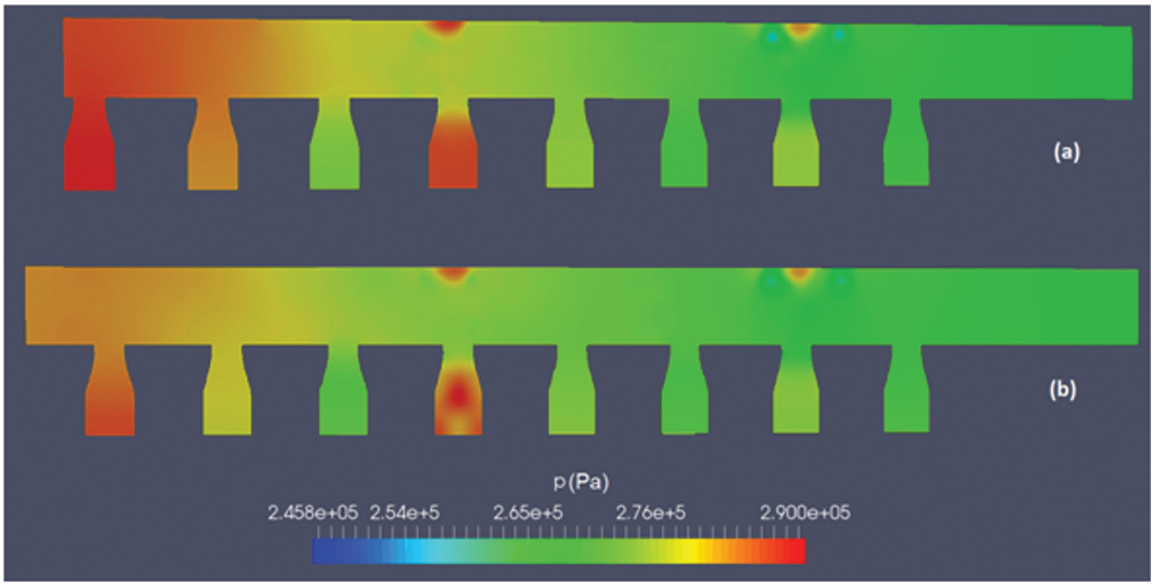

Figure 7. Pressure Distribution at 261 CA° (**a.** Original Manifold; **b.** Manifold with Dead End).

increases at the blind end and also a pressure build-up occurs in the cylinder connection pipes near the blind end. However, this pressure build-up decreased dramatically if a dead end is added to the exhaust manifold. In addition, this decrease in the pressure build-up will also result in better discharging and sweeping of the exhaust gases through the manifold without causing any exhaust backpressure increments or without losing any torque before the turbocharger.

Figure 8 shows the pressure variation inside the manifold after an increase of 79°CA with respect to the casein Figure 5, which corresponds to a crank angle slightly prior to the closure of exhaust valves in cylinder 5. As seen in Figure 8, an unexpected pressure build-up still remains in the interconnection pipe of cylinder 5in the exhaust manifold with a dead end. This build-up is potentially due to the general performance characteristics of cylinder 5, which are relatively low in comparison with the other cylinders. it is stated by Ozsoysal [4–5], the power output and maximum combustion pressure of cylinder 5 are lower than other cylinders.

Similar observations about the pressure distributions in the simulated exhaust manifolds can be made for the

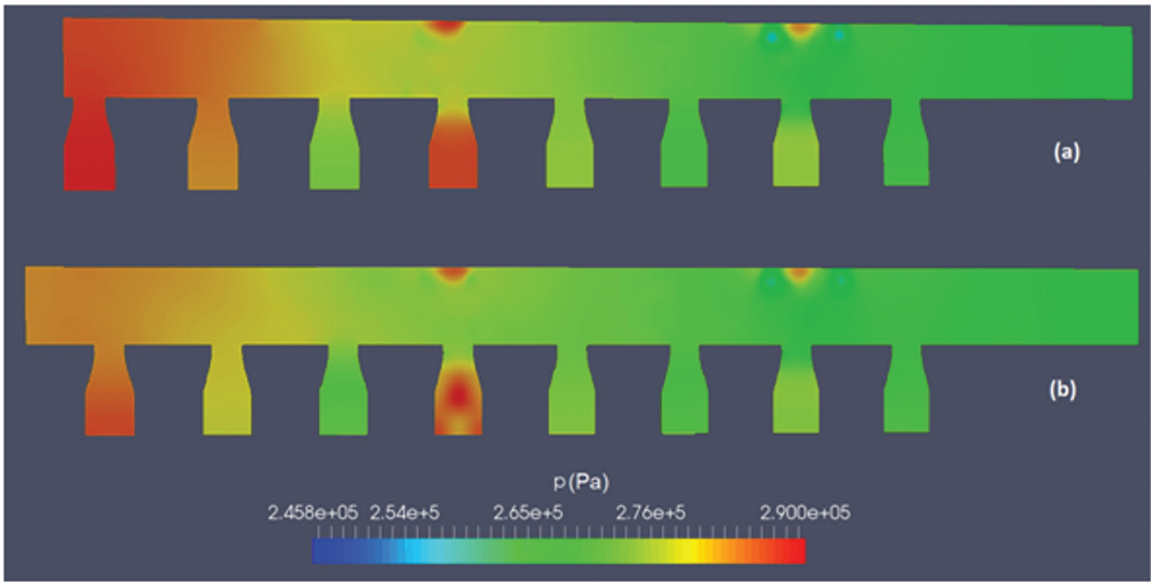

Figure 8. Pressure Distribution at 331 CA° (**a**. Original Manifold; **b**. Manifold with Dead End).

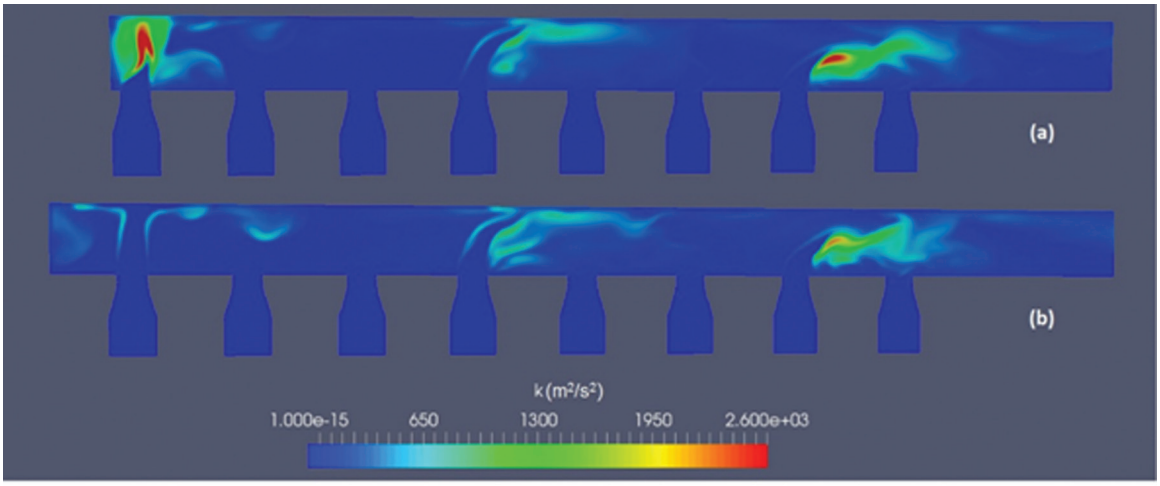

Figure 9. Turbulence Kinetic Energy at 331 CA° (**a**. Original Manifold; **b**. Manifold with Dead End).

turbulence kinetic energy variations. Figure 9 shows the turbulence kinetic energy variation inside the simulated exhaust manifold for the same crank angle in Figure 8. As it can be observed in Figure 9, the turbulence kinetic energy level in the exhaust manifold without a dead end is significantly higher than the one in the exhaust manifold with a dead end. The addition of the dead end has resulted in an increase of the volume at the blind end providing a decrease of the turbulence formation in that area. Moreover, a better uniform flow occurred in the exhaust manifold with the addition of the dead end that leads the turbulence kinetic energy values in the manifold to decrease.

Lastly, Figure 10 shows the kinetic energy variation in the exhaust manifold after an increase of 88^{0}CA with respect to Figure 9. At 419^{0}CA, the blind end next to cylinder 8 still sustains a highly turbulent characteristic for the exhaust manifold without a dead end. This high kinetic energy formed at the blind end causes an increase of the pressure loss in the manifold.

In this study, the aim of adding a dead end at the blind end of the exhaust manifold has been to investigate the impacts of a dead end on the pressure and turbulence kinetic energy variations within the manifold. It is observed that the high pressure values in the cylinder connecting pipes cause some backflows towards the cylinders from the exhaust manifold. In such situation, a satisfactory sweeping of residual gases cannot be guaranteed. Moreover, when a dysfunction occurs in the cylinders, it may unexpectedly cause failure of or even be hazardous to the engine. The addition of a dead end is one of the rational solutions for preventing the

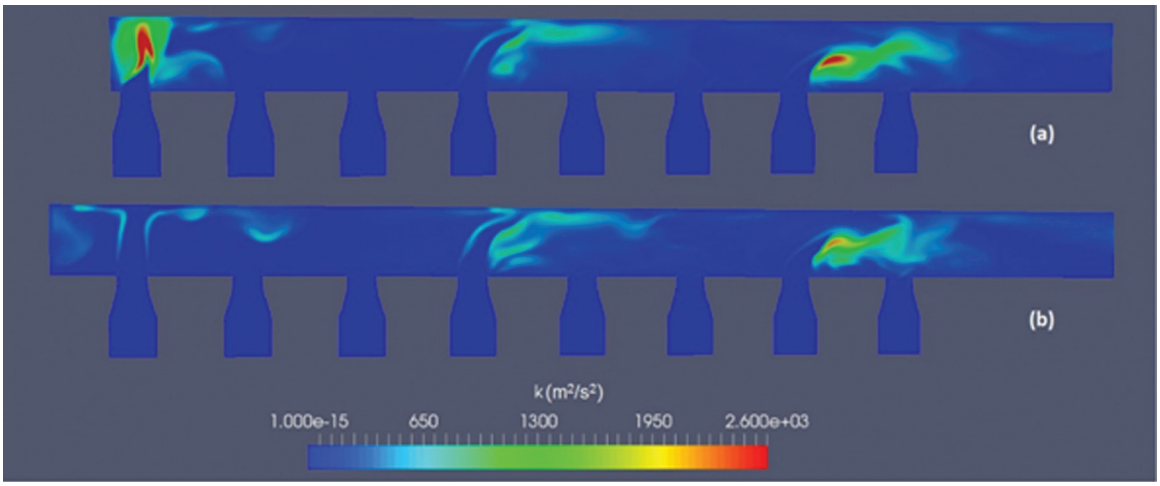

Figure 10. Turbulence Kinetic Energy at 419 CA° (**a**. Original Manifold; **b**. Manifold with Dead End).

exhaust backflow to cylinder due to the unsteady flow in the manifold. The results here clearly reveal the importance of such a dead end connected to the exhaust manifold of a high-speed marine diesel engine.

The pressure values at the blind end of the exhaust manifold with a dead-end remain lower than the pressure values in the same area of the exhaust manifold without a dead-end. Decreases in the pressure values within the cylinder connection pipes were observed with respect to the variations of the pressure distribution. When the exhaust valves open, the encounter of discharging exhaust gases from the cylinders with a lower pressure induces the gases to discharge more easily. This helps to increase the volumetric efficiency of the cylinders, thus increasing the efficiency of the engine.

The addition of the dead end also leads to a decrease in the turbulent kinetic energy values within the exhaust manifold as well as a uniform flow through the manifold to the turbocharger. This, in turn, enables a higher efficiency of the turbocharger.

As the distance between the cylinders is the most important factor determining the geometry of the manifold, the length of the added dead end has been chosen to be half the distance between the cylinders. Although this added dead end regulates the pressure distribution in the manifold, the desired level of improvement has not been achieved. The performance characteristics of the manifold can be further improved by minimizing the power loss seen in the cylinder 5 by performing an optimization study on the length of the added dead end.

CONCLUSION

In this study, an exhaust manifold for a V-16-cylinder marine diesel engine with and without the extensional dead end has been investigated. The following conclusions have been drawn by the comparison between simulation results of an exhaust manifold modeled with and without a dead end. First of all, 3D time-dependent calculations have been employed to obtain the flow structure within an exhaust manifold without a dead end of a marine diesel engine and the resulting flow structure is in agreement with the experimental data. It has been observed that the exhaust gases, with high temperature and velocity, induce considerable turbulence kinetic energy because of the geometric structure of the exhaust manifold without a dead end. The exhaust gases discharging from the cylinders according to the firing order affect the flow pattern as well as the pressure variation and distribution throughout the exhaust manifold. The peak values of pressure waves around the valve area during EVO causes the sweeping phase of the cylinder to be adversely affected.

The dead end was thus extended at the blind end of the manifold to regulate the pressure distribution throughout the exhaust manifold. This dead end extension significantly influences the regulation of the pressure distribution within the exhaust manifold by reducing the pressure values in the cylinder connecting pipes, which are particularly located near the blind end. In addition, it attenuates the flow by means of reflecting the pressure waves from the walls thus causing smoother pressure variations throughout the manifold and interconnection pipes and helping to decrease the turbulence, especially at the blind end side. It is considered that any optimized dead end geometry will further improve the performance characteristics of the cylinders.

NOMENCLATURE

p	pressure, Pa
t	Time, sec
v	Volume,
f_b	Body forces

T	Temperature, °C
C_p	Specific heat, kJ / kg °C
R	Gas constant
k	turbulent kinetic energy
$\dot{q}_v$	unit of heat transfer for unit volume

Greek symbols

β_1	constant of turbulence model
β_2	constant of turbulence model
β^*	constant of turbulence model
σ_{k1}	constant of turbulence model
σ_{k2}	constant of turbulence model
$\sigma_{\omega 1}$	constant of turbulence model
$\sigma_{\omega 2}$	constant of turbulence model
ε	turbulent dissipation
ω	specific rate of dissipation
Φ	dissipation term
Ψ	dissipation term

Subscripts

1*D*	One dimensional
3*D*	Three dimensional
CA	Crank angle, degree
CFD	Computational fluid dynamics
C	Cylinder
DPF	Diesel particulate filter
EVC	Exhaust valve closing
EVO	Exhaust valve opening
RANS	Reynolds averaged Navier Stokes
RPM	Revolution per minute
SCR	Selective catalytic reduction
SI	Spark ignition
SST	Shear stress transport

AUTHORSHIP CONTRIBUTIONS

Authors equally contributed to this work.

DATA AVAILABILITY STATEMENT

No new data were created in this study. The published publication includes all graphics collected or developed during the study.

CONFLICT OF INTEREST

The author declared no potential conflicts of interest with respect to the research, authorship, and/or publication of this article.

ETHICS

There are no ethical issues with the publication of this manuscript.

REFERENCES

[1] Renberg U, Ångström HE, Fuchs L. CA Comparative Study Between 1D and 3D Computational Results for Turbulent Flow in an Exhaust Manifold and in Bent Pipes. (SAE Paper No 2009-01-1112) 2009. [CrosRef]

[2] Zhong W, He Z, Jiang Z, Huang Y. CA flow field analysis of pulse converter exhaust manifold of diesel engines. Advanced Materials Research 2012;468-471:1693–1696. [CrosRef]

[3] Wang Y, Semlitsch B, Mihaescu M and Fuchs L. Flow structures and losses in the exhaust port of an internal combustion engine. International Mechanical Engineering Congress and Exposition - IMECE2013-64610 2013. [CrosRef]

[4] Ozsoysal OA. Analytical and Experimental Investigation of High Speed Marine Diesel Engines. Doctoral Dissertation, İstanbul Technical University, Turkey, 1991. (Turkish)

[5] Ozsoysal OA. Investigation of the Engine Data by Comparing the Experimental Test with the Results of Analytical Model 1993. (SAE Paper No. 930611). Paper presented at the meeting of International Congress and Exposition, Detroit, Michigan. [CrosRef]

[6] Luján JM, Galindo J, Serrano JR, Pla B. A methodology to identify the intake charge cylinder-to-cylinder distribution in turbocharged direct injection diesel engines. Measurement Science and Technology 2008;19:065401. [CrosRef]

[7] Xu J, Zhou S. Analysis of flow field for automotive exhaust system based on computational fluid dynamics. The Open Mechanical Engineering Journal 2014;8:587–593. [CrosRef]

[8] Nursal RS, Hashim AH, Nordin NI, Hamid MAA, Danuri MR. CFD analysis on the effects of exhaust backpressure generated by four-stroke marine diesel generator after modification of silencer and exhaust flow design. ARPN Journal of Engineering and Applied Sciences 2018;12:4.

[9] Ardabili SF, Najafi B, Shamshirband S, Bidgoli BM, Deo RC, Chau KW. Computational intelligence approach for modeling hydrogen production: a review. Engineering Applications of Computational Fluid Mechanics 2018;12:438–458. [CrosRef]

[10] Zhang J, Zhang X, Wang T, Hou X. A numerical study on jet characteristics under different supercritical conditions for engine applications. Applied Energy 2019;252:113428. [CrosRef]

[11] Wu S, Zhou D, Yang W, Implementation of an efficient method of moments for treatment of soot formation and oxidation processes in three-dimensional engine simulations. Applied Energy 2019;254:113661. [CrosRef]

[12] Zhang C, Hu B, lai C, Zhang H, Qin L, Leng X, Huang W. Simulation Study of 1D-3D Coupling

for Different Exhaust Manifold Geometry on a Turbocharged Gasoline Engine (SAE Paper No 2018-01-0182) 2018. [CrosRef]

[13] Payri F, Reyes E, Galindo J. Analysis and modeling of the fluid-dynamic effects in branched exhaust junctions of ICE. Journal of Engineering for Gas Turbines and Power 2001;123:197–203. [CrosRef]

[14] Emara K, Emara A, Razek EA. CFD Analysis & Experimental Investigation of a Heavy Duty D.I. Diesel Engine Exhaust System. Paper presented at the meeting of the International Mechanical Engineering Congress and Exposition 2016, Phoenix, Arizona, USA. [CrosRef]

[15] Hinterberger C, Olesen M. Automatic Geometry Optimization of Exhaust Systems Based on Sensitivities Computed by a Continuous Adjoint CFD Method in OpenFOAM 2010. (SAE Paper No. 2010-01-1278). SAE International. [CrosRef]

[16] Siqueira C, de La R, Kessler MP, Rampazzo R, Cardoso DA. Three Dimensional Numerical Analysis of Flow Inside Exhaust Manifold 2006. (SAE Paper No. 2006-01-2623). Paper presented at the meeting of XV Congresso e Exposição Internacionais da Tecnologia da Mobilidade, São Paulo, Brasil.

[17] Xu P, Jiang H, Zhao X. CFD analysis of a gasoline engine exhaust pipe. Journal of Applied Mechanical Engineering 2016;5:2. [CrosRef]

[18] Umesh KS, Pravin VK, Rajagopal K. CFD analysis and experimental verification of effect of manifold geometry on volumetric efficiency and back pressure for multi-cylinder si engine. International Journal of Engineering & Science Research 2013;3: 342–353.

[19] Rajadurai S, Paulraj M, Victor A. Effective Methodology for Backpressure Prediction of Hot Exhaust Gas in Cold Flow Bench Test 2016. (SAE Paper No. 2002-01-0901). [CrosRef]

[20] Ma Z, Chen X, Gao D, Xu B. The CFD analysis of exhaust runner for GW15 gasoline engine. Advanced Materials Research 2013;655-657:326–331. [CrosRef]

[21] Pulliam TH, Zingg DW. Fundamental algorithms in computational fluid dynamics. Scientific Computation 2014:59–74. [CrosRef]

[22] Menter FR. Improved two-equation k-omega turbulence models for aerodynamic flows. ASA STI/ Recon Technical Report N. 1992

[23] Lee CH. Rough boundary treatment method for the shearstresstransport k - ω model, Engineering Applications of Computational Fluid Mechanics 2018;12:261–269. [CrosRef]

[24] Launder BE, Spalding DB. The numerical computation of turbulent flows. Computer Methods in Applied Mechanics and Engineering 1974;3:269–289.

[25] Wilcox DC. Reassessment of the scale-determining equation for advanced turbulence models. AIAA Journal 1988;26:1299–1310. [CrosRef]

[26] Davidson L. Fluid mechanics, turbulent flow and turbulence modeling 2014. Master of Science Dissertation, Chalmers University of Technology, Sweden.